ELSEVIER

Applied Acoustics, Vol. 52, No. 3/4, pp. 273–288, 1997

Printed in Great Britain
PII: S0003-682X(97)00031-5 0003-682X/97 $17.00+0.00

Low-Frequency Airborne Sound Transmission through Single Partitions in Buildings

A. Osipov,[a] P. Mees[b] and G. Vermeir[a]

[a]Laboratory of Building Physics, Department of Civil Engineering, KU Leuven, Celestijnenlaan 131, 3001 Leuven, Belgium
[b]Daidalos Bouwfysisch Ingenieursbureau, Albrecht Rodenbachstraat 71, 3010 Leuven, Belgium

(Received 27 September 1996; revised version received 23 December 1996; accepted 17 April 1997)

ABSTRACT

The low-frequency (20–250 Hz) airborne sound transmission of single partitions is investigated. Three theoretical models are used for the prediction: an infinite plate model, a baffled plate model and a room–plate–room model. The calculation models are verified by detailed comparisons with experimental results obtained in the laboratory. A parametric study is carried out to examine the influence of the dimensions of the room and the partition. The results demonstrate the strong modal behaviour of the low-frequency sound transmission. As a result, the low-frequency sound insulation depends not only on the properties of the test wall but also on the geometry and the dimensions of the room–wall–room system. In general, the large variation of the low-frequency insulation compromises the accuracy of prediction of the sound insulation in situ. © *1997 Elsevier Science Ltd.*

Keywords: Low frequencies, sound insulation, buildings.

INTRODUCTION

The problem of sound transmission in buildings at low frequencies is becoming of increasing practical[1] and theoretical interest[2–4] due to the growing impact of low-frequency indoor and outdoor noise sources.[5,6] The low-frequency range is not included in current standards on sound insulation measurements. Work by different authors[2–4,7] showed that the sound

reduction index in this range depends on several parameters, e.g. the room's dimensions, the reverberation time, the position of the sound source. Therefore it is very difficult to extrapolate laboratory results to situations with different geometry and dimensions of the rooms or the partition. This paper is aimed at improving the understanding of this problem by means of a detailed analysis of the low-frequency sound transmission through a single partition.

CALCULATION MODELS

The analysis is restricted to airborne sound transmission through plane, rectangular, single-leaf walls. The walls are assumed to be homogeneous, isotropic, and thin compared to the bending wavelength. Harmonic pure bending wave motion according to Kirchhoff's theory is used for the analysis.

The infinite plate model

This is the classical approach based on plane wave transmission through an infinitely extended plate.[8] The sound transmission loss at normal incidence is governed by the mass law:

$$TL_{\mathrm{ML}} = 10\log[1 + (\omega m_{\mathrm{p}}/2\rho c)^2] \tag{1}$$

where m_{p} is the mass per unit area of the wall.

For oblique incidence there is an increased sound transmission at the critical frequency, which depends on the mass and the stiffness of the wall. The sound transmission coefficient is given by

$$\tau_\alpha = |\ 1 + \mathrm{i}(\omega m_{\mathrm{p}} \cos\alpha/2\rho c)[1 - (k^4/k_b^4)\sin^4\alpha]\ |^{-2} \tag{2}$$

where α is the angle of incidence, k is the wave number in the air, and k_{b} is the free bending wave number.

The random incidence sound transmission loss (TL_{R}) is obtained by integrating over the angles of incidence:

$$TL_{\mathrm{R}} = 10\log\left(\int_{0^\circ}^{78^\circ} \tau_\alpha \sin 2\alpha \, \mathrm{d}\alpha\right)^{-1} \tag{3}$$

The baffled plate model

A plane wave of unit amplitude is incident on a finite sized plate mounted in an infinitely extended, rigid baffle. The sound pressure radiated by the plate is expressed in terms of the Huygens integral:[9]

$$P(x_1, y_1, z_1) = -\frac{i\omega\rho}{2\pi}\int\int_s v(x', y')\frac{\exp(ikR)}{R}\,ds \tag{4}$$

where v is the particle velocity on the plate surface, R is the distance from the surface element ds to the observation point, and s is the area of the plate.

The difference between the total sound pressures on the two sides of the plate in the plane of the baffle (x_1,y_1,$z_1 = 0$) is substituted into the bending wave equation of the plate. The transverse velocity of the plate is expanded as a summation over the modeshapes of the plate *in vacuo*. The radiation impedances of the individual modeshapes of the plate are calculated numerically. In the equations of motion the cross-modal radiation impedance terms are neglected. This simplification is reported to be well adapted in the case of sound radiation of bending waves into a light fluid.[10] Finally, the transmission coefficient is calculated as the ratio of the acoustic power radiated at the receiving side to the power incident on the plate.

The room–plate–room model

In this model, the full coupling between the bending modes of the plate and the modes in the emitting and receiving room is taken into account.[7] The analysis is restricted to a rectangular geometry, which allows for an analytical modal decomposition of the displacement of the panel and the sound field in both rooms. The sound pressure at any point (x,y,z) in a room fulfils the Helmholtz equation and is written as a summation of oppositely travelling plane waves:

$$\begin{aligned} P(x, y, z) &= \sum_m \sum_n [\exp(-ik_{zmn}z)A_{mn} + \exp(ik_{zmn}z)B_{mn}]\phi_{mn}(x, y) \\ \phi_{mn}(x, y) &= \cos\left(\frac{m\pi}{L_x}x\right)\cos\left(\frac{n\pi}{L_y}y\right) \qquad k_{zmn}^2 + \left(\frac{m\pi}{L_x}\right)^2 + \left(\frac{n\pi}{L_y}\right)^2 = k^2 \end{aligned} \tag{5}$$

where A_{mn} and B_{mn} are the unknown pressure amplitudes, L_x,L_y,L_z are the room dimensions, m,n are summation indices, and k is the wave number in the air. In expression (5), the room boundaries normal to the separating wall are assumed to be rigid.

The transverse displacement at any point (x,y) on the plate fulfils Kirchhoff's thin plate bending wave equation and is expanded as a modal summation over the plate's eigenfunctions *in vacuo*:

$$\xi(x, y) = \sum_m \sum_n C_{mn} \psi_{mn}(x, y) \tag{6}$$

where C_{mn} are the unknown plate displacement amplitudes.

The unknown plate and pressure amplitudes are solved from the plate equation of motion and from the continuity conditions between the sound fields and the plate surfaces.

The difference between the three models is illustrated by the results presented in Figs 1 and 2. The airborne sound transmission loss is plotted for walls constructed of four different materials: heavy concrete, lightweight concrete, glass, and PVC. The material data used in the calculations are given in Table 1.

The infinite plate theory predicts a smooth variation of the sound transmission loss as a function of frequency, with a pronounced dip at the critical frequency of the panel. The numerical results calculated with the baffled plate model show an irregular sound transmission function, with violent peaks and dips due to the modal behaviour of the finite sized plate.

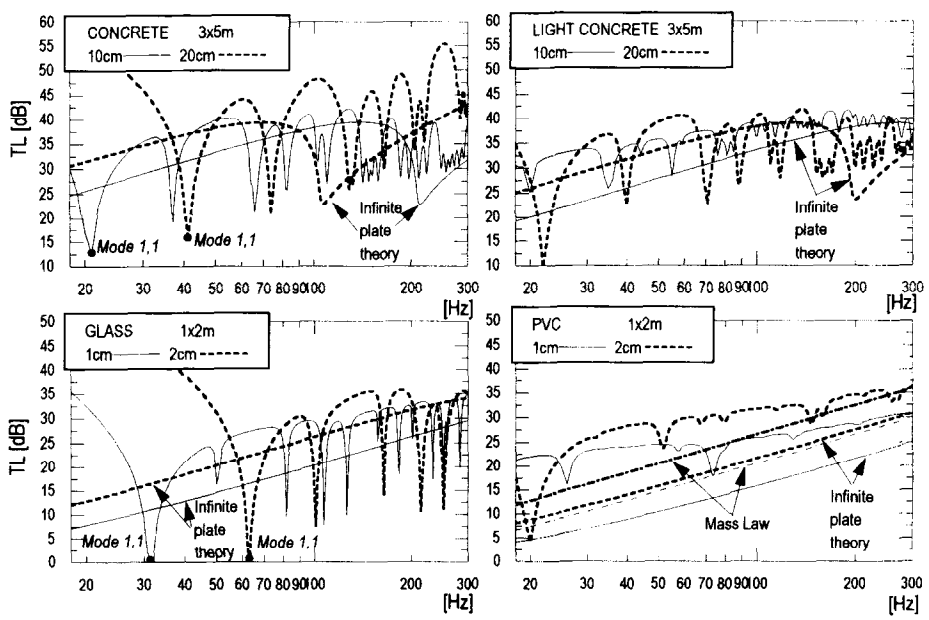

Fig. 1. Predicted transmission loss of different walls. The infinite plate theory and the baffled plate model (simply supported).

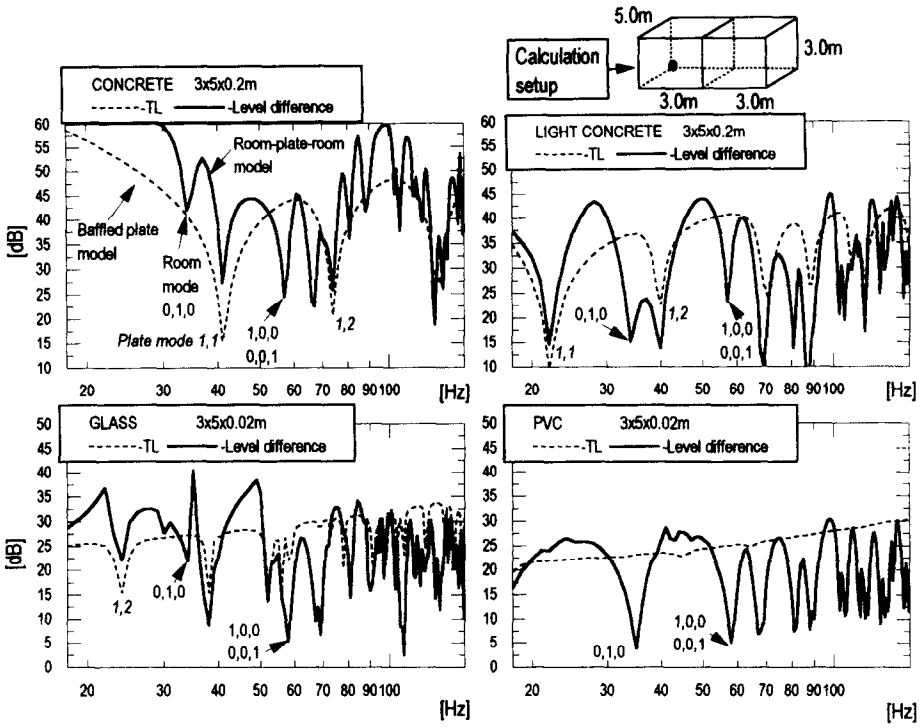

Fig. 2. Predicted transmission loss and level difference. Modal approach: the baffled plate model (simply supported) and the room–plate–room model.

The results calculated with the room–plate–room model show similar characteristics, with additional modulations due to the modal behaviour of the two rooms.

EXPERIMENTAL SETUP

As a validation of the calculation models, measurements were carried out in the transmission rooms of the acoustics laboratory of the KU Leuven and in the laboratory of the Belgian Building Research Institute (CSTC/WTCB, further called CSTC). The rooms at the KU Leuven are of identical shape,

TABLE 1
Material Properties of the Walls

Material	*Young's modulus (N/m^2)*	*Density (kg/m^3)*	*Loss factor*	*Poisson's ratio*
Concrete	2.0 E10	2300	0.015	0.2
Light concrete	3.0 E9	1200	0.02	0.2
Glass	7.2 E10	2490	0.003	0.25
PVC	3.7 E9	1440	0.04	0.4

with a slightly inclined test partition, and with a volume of 85 m^3 each. The rooms at the CSTC are perfectly rectangular, with volumes of 50 and 49 m^3.

The partitions tested were a calcium silicate brick wall (3×3.3×0.1 m) and a thick glass plate (1.48×1.25×0.019 m). The brick wall was tested in the KU Leuven laboratory only and the glass plate was tested in both laboratories. The glass plate was mounted in glazing test frames according to ISO 140-3:1995.[11]

Additional experiments were performed in a scale model (1:5) of two adjacent rooms (2 m^3) separated by a glass plate (1.285×1.21×0.019 m).

The rooms were exited by a loudspeaker mounted in a back corner or suspended close to the back wall. The sound pressure levels were measured in narrow frequency bands (FFT mode, 0.5 Hz resolution, 1–400 Hz range) and in 1/3 octave bands in 33 fixed microphone positions. The measurements were carried out in both directions. The sound reduction index (SRI) was calculated according to ISO 140-3:1995.

In the figures we use TL (transmission loss) as an abbreviation for the data measured in narrow frequency bands.

The modulus of elasticity of the partition materials was derived from measurements of the resonance frequencies of the free-free beam samples.[12]

The total loss factors of the partitions were measured with a decay rate technique. The reverberation time of the mounted specimens was calculated on the Schroeder's decay curve derived from a measurement of the impulse response of the test wall.

The modal frequencies of the mounted partitions were obtained from the measured frequency response function (a hammer excitation).[13] The results indicate that the boundary conditions of the tested partitions were very close to simply supported. Therefore these boundary conditions are considered for the predictions.

RESULTS

The calcium silicate brick wall

Figure 3 shows the measured response of both rooms and the calcium silicate test wall. The sound field in the emitting room is dominated exclusively by room modes (Fig. 3(A)); the sound field in the receiving room is determined by both plate and room modes (Fig. 3(C)). With airborne sound excitation, the acceleration of the plate is composed of a resonant part and a non-resonant part enforced by the sound field in the emitting room. The additional peaks in the response of the plate when passing from mechanical to acoustical

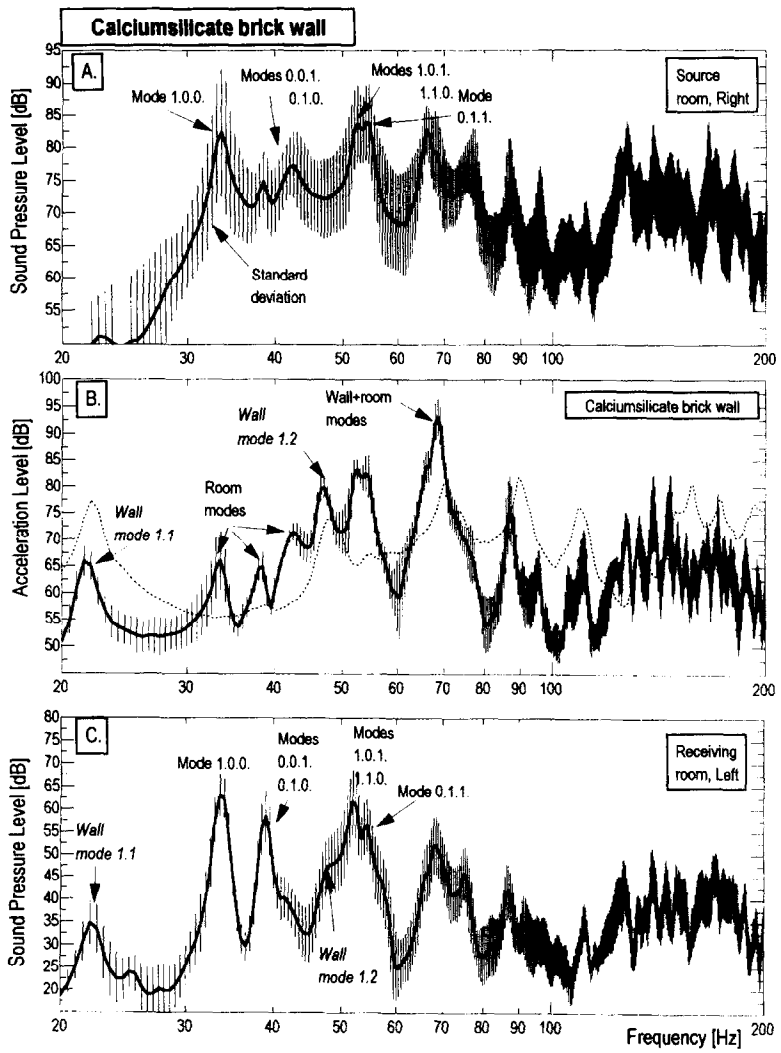

Fig. 3. KU Leuven transmission rooms. Measured sound pressure and acceleration levels. —, measurements (airborne source); · · · · · ·, response of the wall due to mechanical excitation.

excitation are clearly identified (Fig. 3(B)). The calculation results indicate that the room–plate–room model provides better agreement with measurement results compared to the infinite or baffled plate models (Fig. 4). Deviations at individual frequencies can be very large, but the influence of room modes on the detailed sound transmission loss is correctly predicted.

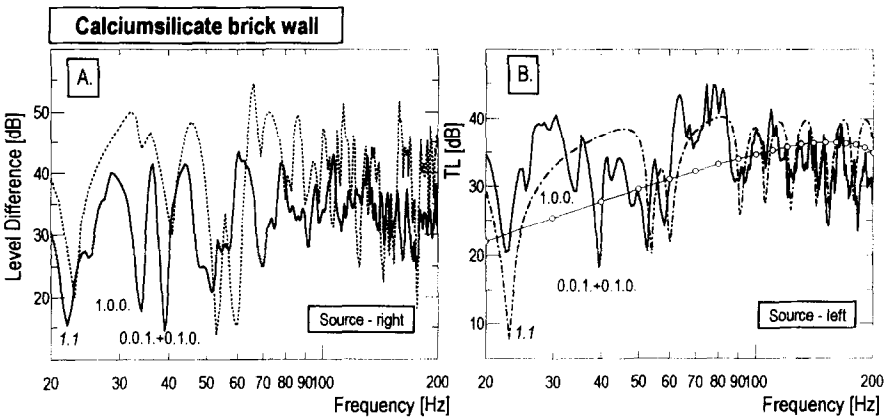

Fig. 4. KU Leuven transmission rooms. Measured and predicted sound pressure level difference and transmission loss (TL). ——, measurements; —○—, infinite plate theory; - - - - -, baffled plate model; · · · · · ·, room–plate–room model.

The glass plate

The glass plate was tested at the laboratories of the KU Leuven and the CSTC. Figure 5 shows that the agreement between the measurements in both laboratories is reasonable for frequencies above 80 Hz. The small deviations in this range can be attributed to minor differences in mounting and test conditions. However, a large difference of the measured sound reduction indices, up to 25 dB, is observed in the frequency range from 45 to 65 Hz. The measurement is confirmed by calculations (Fig. 6). In the frequency range from 50 to 60 Hz, a very high sound insulation is predicted for the laboratory of the CSTC, whereas a very low value is predicted for the laboratory of the KU Leuven. This result can be explained by considering

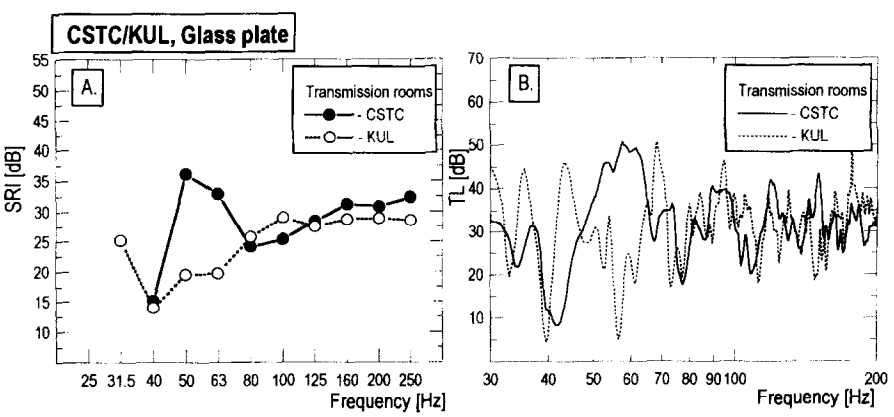

Fig. 5. CSTC/KU Leuven transmission rooms. Measured SRI and transmission loss (TL).

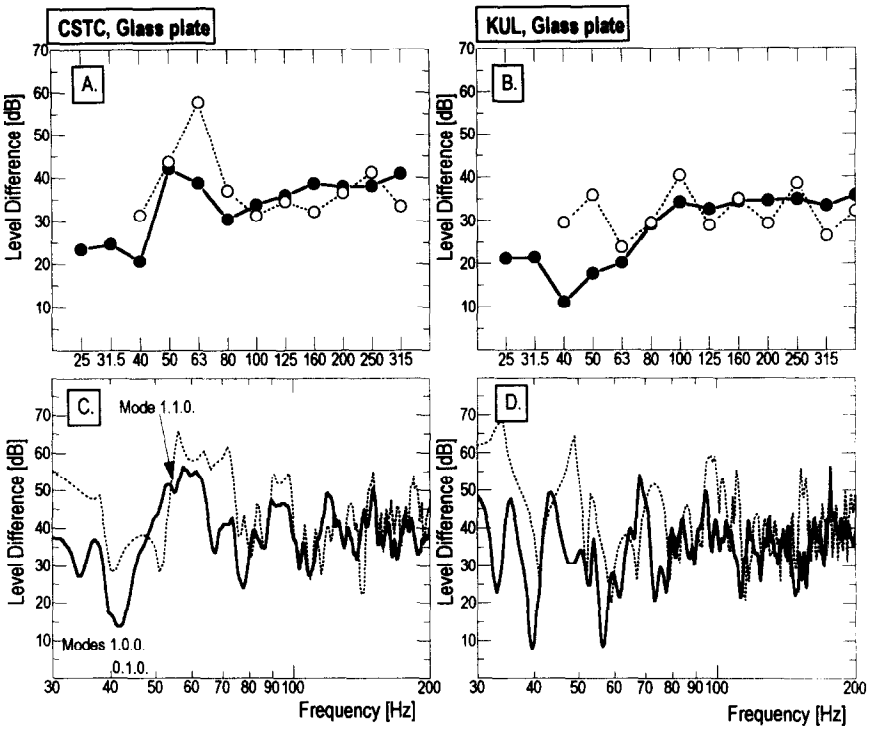

Fig. 6. CSTC/KU Leuven transmission rooms. Measured and predicted sound pressure level difference. —●—, measurements; —○—, ·····, prediction.

the measured narrow band response of the transmission rooms at the CSTC and the KU Leuven (Fig. 7). In the receiving room of the CSTC, one tangential mode (1.1.0., 55 Hz) can be identified in the frequency range from 50 to 60 Hz (Fig. 7(B)). Moreover, the response of this tangential mode is very weak. In the receiving room of the KU Leuven, four modes are present in the same frequency range (Fig. 7(D)).

A numerical experiment is performed in order to explain the weak response of the tangential mode (1.1.0.) in the laboratory of the CSTC. The sound pressure level difference is calculated for different positions of the test partition in the laboratory wall separating the two rooms (Fig. 8). In the first case, the test partition is placed in the middle of the separating wall. This position corresponds to a pressure node of the tangential mode (1.1.0.) of the receiving room, which results in a very weak excitation of the sound field. In the third case, the test partition is located close to the corner, and the tangential mode (1.1.0.) in the receiving room is excited to its fullest extent.

The difference between the two laboratories is also observed in the measured acceleration level of the glass plate when excited by airborne sound (Fig. 9). As indicated previously, this response is enforced by modes in the

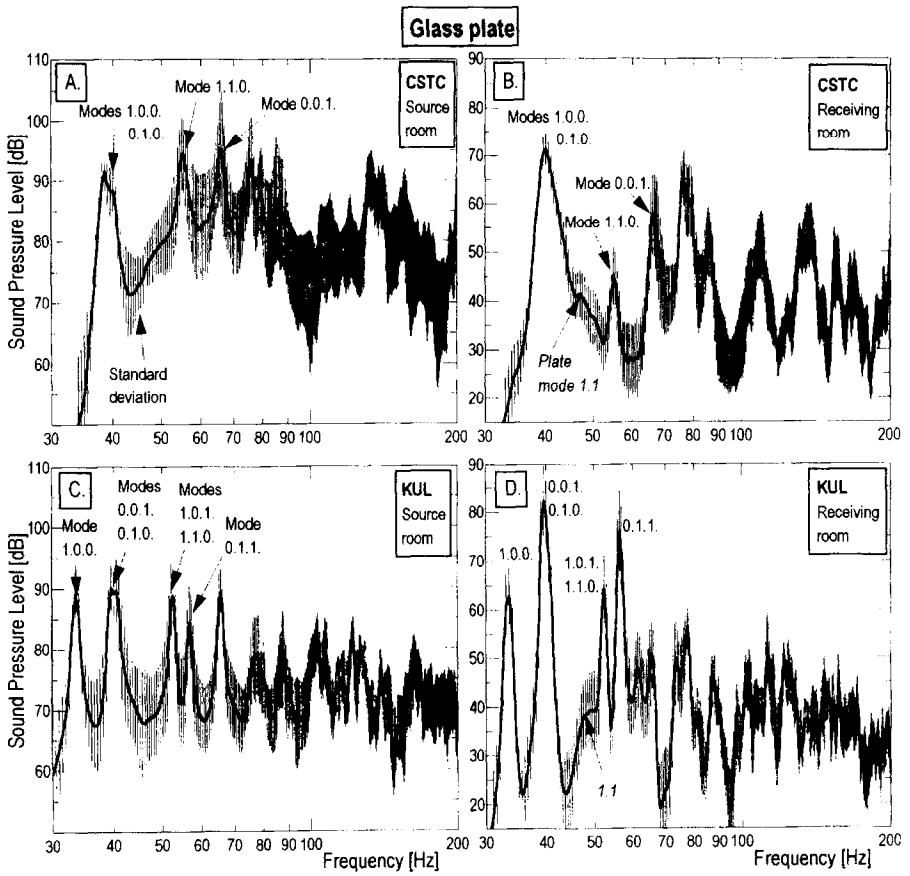

Fig. 7. CSTC/KU Leuven transmission rooms. Measured sound pressure levels. ——, measurements.

emitting room. If one looks at the detailed spectrum of the response, the different characteristic frequencies of the rooms modes at the CSTC and the KU Leuven can be clearly observed.

Figure 10 shows the predicted and the measured radiation efficiency (in dB) of the glass plate. The values of the radiation efficiency σ are derived from the radiated acoustic intensity I and the surface velocity v of the plate using the following equation.

$$\sigma = \frac{I}{\rho c < v^2 >} \tag{7}$$

The glass plate is excited directly by airborne sound in the source room. The predicted results are obtained from Maidanik's formulation,[14] Leppington's modified expression,[15] the baffled plate model (no cross-coupling

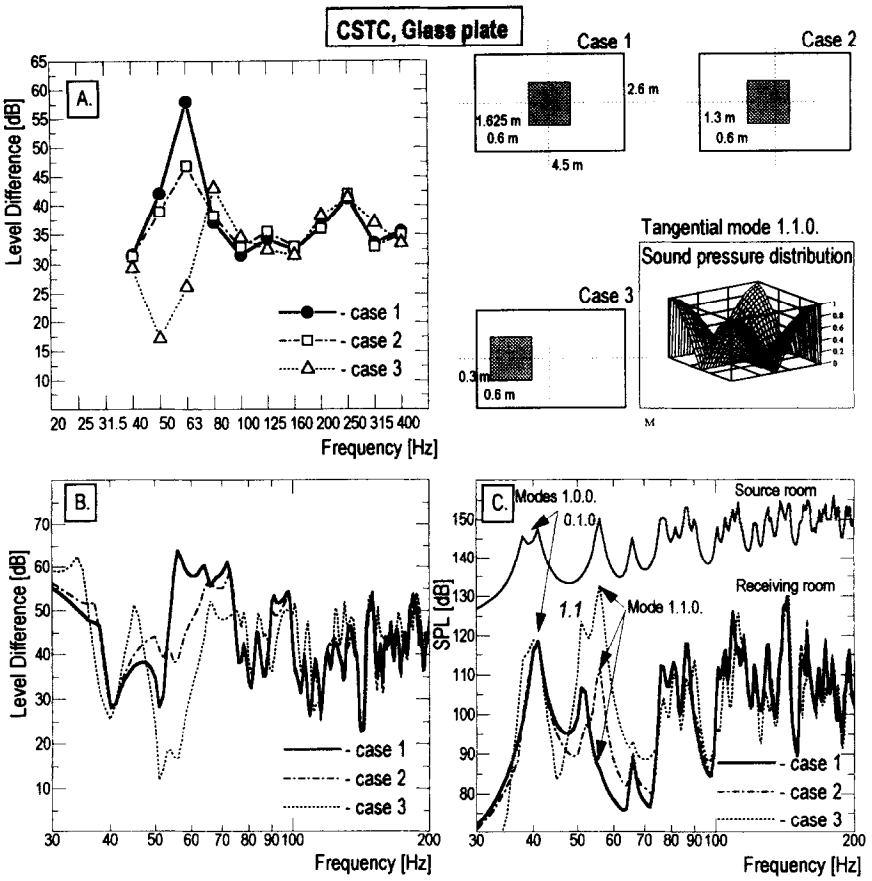

Fig. 8. CSTC transmission rooms. Calculated sound pressure level difference for different positions of the test partition in the laboratory wall separating the two rooms.

terms), and the room–plate–room model. These results allow us to point out the following interesting comments. Above 200 Hz, the approaches of Maidanik, Leppington, and the baffled plate model give an average radiation factor that approximates the main trend of the measurement. Below 200 Hz these three methods have problems in describing accurately the variation of the radiation efficiency. In this range the room–plate–room model gives a better agreement with the measurements. These results demonstrate that the sound radiation of a panel is determined by the properties of both the panel and the room.

In order to vary the dimensions of the room to extreme values, an additional test was carried out in a scale model. Figure 11 shows the predicted results of the baffled plate model and the room–plate–room model compared to the experimental data. The agreement between the measured and the predicted results is satisfactory. Additional peaks and dips in the results

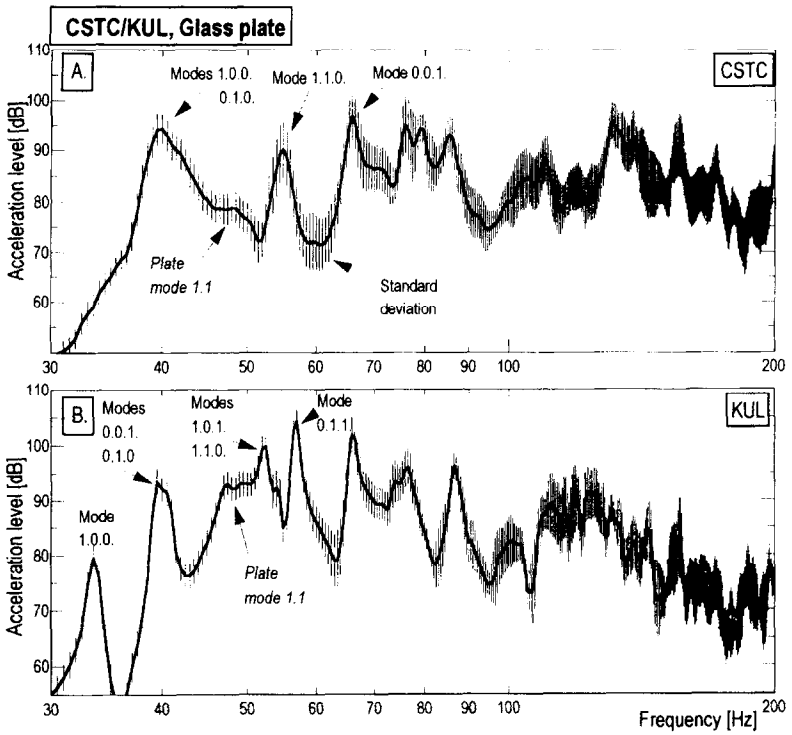

Fig. 9. CSTC/KU Leuven transmission rooms. Measured acceleration level of the glass plate. Airborne excitation.

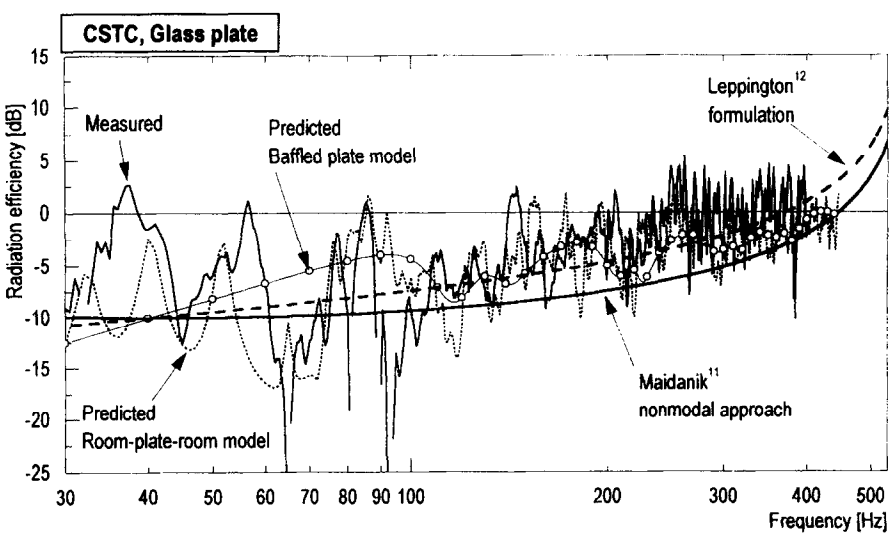

Fig. 10. CSTC transmission rooms. The height of the receiving room is increased by a factor of 2. Predicted and measured radiation efficiency. ——, measured; ——, - - - -, —○—, ·····, predicted. Simply supported boundary conditions of the plate are assumed.

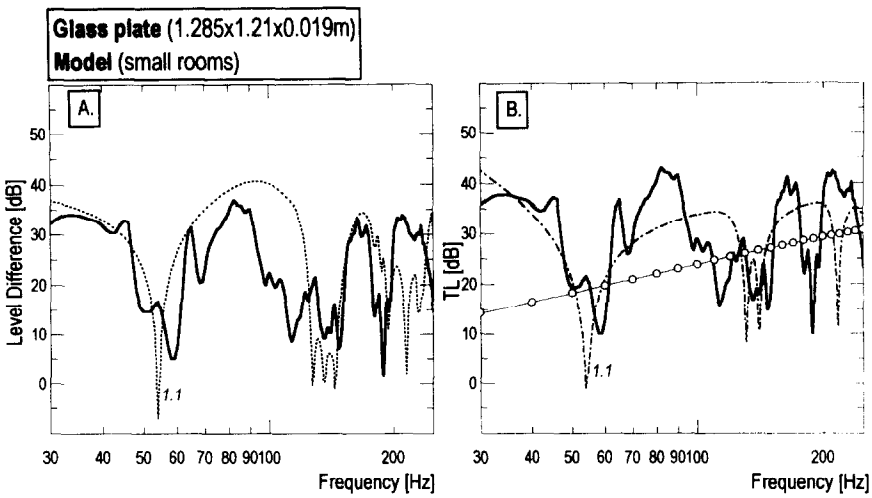

Fig. 11. Model (small rooms). Measured and predicted sound pressure level difference and transmission loss (TL). ——, measurements; —o—, infinite plate theory; - - - - -, baffled plate model; · · · · · ·, room–plate–room model.

predicted by the room–plate–room model are apparent only above 120 Hz, the characteristic frequency of the first mode of the volume.

In conclusion, the room–plate–room calculation model can be considered as sufficiently accurate for predicting the low-frequency sound transmission and therefore this model is applied to the parametric study.

Parametric study

Numerical experiments were carried out to examine the influence of the dimensions of the room and the partition on the sound transmission loss. In the first experiment, shown in Fig. 12, the back wall of the receiving room is moved: this affects selected modes of the receiving room only. In the second experiment, shown in Fig. 13, the width of the partition is varied: this affects selected modes of the emitting and receiving room and all modes of the partition. In both experiments, the reverberation time of the emitting and receiving rooms is 2.5 s and 1.0 s, respectively. The spatial average of the sound pressure is calculated by integrating over the whole room volume. This value is subsequently averaged over the 1/3 octave bands and full octave bands for the setup shown in Fig. 13. The sound reduction index (SRI) is calculated according to ISO 140-3:1995. Calculated results show that the SRI varies over a wide range. Within the small frequency range considered, the SRI ranges from 20 to 50 dB for the heavy concrete partition and from 20 to 45 dB for the lightweight concrete partition. The variations in individual 1/3 octave bands are up to 15 dB. In full octave bands the variations range from 2 to 6 dB.

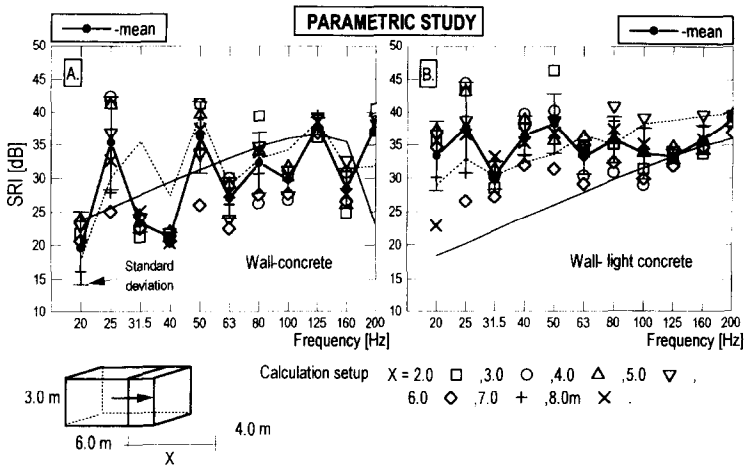

Fig. 12. Predicted SRI. Wall thickness 10 cm. —, Infinite plate theory; ·····, baffled plate model. Symbols: room–plate–room model.

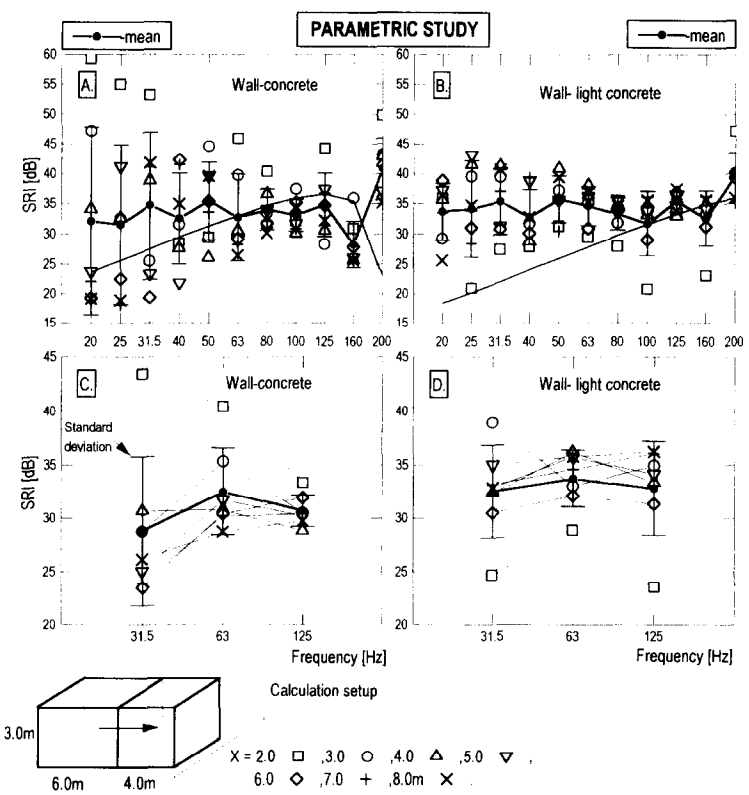

Fig. 13. Predicted SRI. Wall thickness 10 cm. —, Infinite plate theory. Symbols: room–plate–room model. Graphs (A), (B) averaging over 1/3 octave bands; graphs (C), (D) averaging over full octave bands.

The parametric study shows that in the low-frequency range it is very difficult to extrapolate laboratory results to situations with different geometry and dimensions for the rooms or the partition. However, expressing the low-frequency transmission loss in full octave bands (Fig. 13(C) and (D)) minimises the influence of the room's or wall's dimensions.

CONCLUSION

The room–plate–room model, based on an analytical modal analysis of a rectangular geometry, allows for a deterministic calculation of the low-frequency sound transmission between two rooms separated by a wall. This model allows study of the influence of different parameters (the room's dimensions, the reverberation time, the position of the source). Calculation examples showing the influence of some parameters have been presented.

The infinite and baffled plate models are not able to take into account the coupling between the bending modes of the plate and the modes of the room. Therefore, these two models have to be used very carefully in the low-frequency range.

The results show that the sound transmission at low frequencies depends not only on the properties of the test wall but also on the geometry of the room–wall–room system. For rigid, stiff walls both resonant and non-resonant transmission significantly affect the sound insulation. In general, variation in low-frequency insulation compromises the accuracy of a prediction of the sound insulation *in situ*. In our further research we will focus on the validation of the results of the parameter study, by comparing measurements and predictions of the low-frequency sound transmission between rooms with separated panels of varying size and varying bending stiffness.

ACKNOWLEDGEMENT

The authors are grateful to the Belgian Building Research Institute (CSTC/WTCB) and the IWONL Research Foundation for supporting this work. Part of the results included in this paper were presented at Inter-Noise 96.[16]

REFERENCES

1. Pedersen, D. B., Measurement of the low-frequency sound insulation of building components. Technical report DTI 260 3 8016, Phase I,II. DTA Acoustics, Aarhus, Denmark, 1994.

2. Kropp, W., Pietrzyk, A. and Kihlman, T., On the meaning of the sound reduction index at low frequencies. *Acta Acustica*, 1994, **2**, 379–392.
3. Pietrzyk, A., Kropp, W. and Kihlman T., Numerical simulation of low frequency air-borne sound transmission in buildings. Proceedings of CIB W-51 Acoustics. Warsaw, 1994, pp. 156–161.
4. Warnock, A. C. C. and Vorlander, M., Inter-laboratory comparison of low frequency sound transmission—finite element studies. Proceedings of Inter-Noise 93. Leuven, 1993, pp. 929–932.
5. Mathys, J., Low frequency noise and acoustical standards. *Applied Acoustics*, 1993, **40**(3), 185–200.
6. Berglund, B., Hassmen, P. and Soames Job, R. F., Sources and effects of low-frequency noise. *Journal of the Acoustical Society of America*, 1996, **99**(5), 2985–3002.
7. Gagliardini, L., Roland, J. and Guyader, J. L., The use of a functional basis to calculate acoustic transmission between rooms. *Journal of Sound and Vibration*, 1991, **145**(3), 457–478.
8. Heckl, M., The tenth Sir Richard Fairey memorial lecture: sound transmission in buildings. *Journal of Sound and Vibration*, 1981, **77**(2), 165–189.
9. Gurovich, Yu. A., Low-frequency acoustic reduction of a rectangular panel. *Sov. Phys. Acoust.*, 1978, **24**(4), 289–292.
10. Guyader, J. L. and Laulagnet, B., Structural acoustic radiation prediction: expanding the vibratory response on a functional basis. *Applied Acoustics*, 1994, **43**(3), 247–269.
11. ISO/DIS 140-3:1995, Laboratory measurement of airborne sound insulation of building elements. 1995.
12. ASTM E756-83, Standard method for measuring vibration-damping properties of materials. 1983.
13. ISO 7626-5:1994, Vibration and shock—experimental determination of mechanical mobility. Part 5: measurements using impact excitation with an exciter which is not attached to the structure, 1994.
14. Maidanik, G., Response of ribbed panels to reverberant acoustic fields. *Journal of the Acoustical Society of America*, 1962, **34**, 809–826.
15. Craik, R. J. M., *Sound Transmission through Buildings Using Statistical Energy Analysis*. Gover, Hampshire, 1996, p. 92.
16. Osipov, A., Mees, P. and Vermeir, G., Low frequency airborne sound transmission in buildings: single plane walls. Proceedings of Inter-Noise 96. Liverpool, 1996, pp. 1791–1794.